JOURNAL OF CATALYSIS **180,** 44–50 (1998)
ARTICLE NO. CA982235

Influence of Structural Heterogeneity on Selectivity in Fractal Catalyst Structures

Sean P. Rigby[1] and Lynn F. Gladden

Department of Chemical Engineering, University of Cambridge, Pembroke Street, Cambridge, CB2 3RA, United Kingdom

Received March 13, 1998; revised July 2, 1998; accepted July 2, 1998

In the past Monte-Carlo simulations have been used to study the influence of morphological properties of fractal surfaces on the selectivity between competing three-step catalytic reactions. These simulations were conducted using abstract two-dimensional diffusion-limited aggregate models. In an attempt to identify the appropriate properties of a real material that should be represented in a model this previous work has been extended to consider three-dimensional models (cluster-cluster aggregates and the Menger sponge), in order to correlate selectivity with model characteristics which may be related to input from experimental characterisation data, such as that from magnetic resonance imaging. The simulations on three-dimensional models have shown that both the porosity and the mass fractal dimension of the models are important to accurately represent a real porous material; a finding not explicit in previous work in two dimensions. © 1998 Academic Press

INTRODUCTION

Magnetic resonance imaging studies (1–3) have suggested that transport processes within porous catalyst support pellets are influenced by heterogeneities in the spatial distribution of voidage and pore size over macroscopic lengthscales (0.01–10 mm). Analysis of the NMR images using an algorithm employing fractal concepts has shown that the structure of porous catalyst support pellets has a fractal character on the macroscopic scale and that the fractal parameter so-obtained may be correlated with transport properties (3). Results from gas sorption (4) have shown that the geometry of porous catalyst pellets on the microscopic scale can also be fractal in nature.

There is increasing interest in understanding the effects of fractal geometry on catalyst characteristics. In early work Meakin (5) explored the effects of fractal geometry on a simple model of catalyst selectivity. Two dimensional simulations using random walks were carried out on diffusion-limited aggregates (DLAs) to investigate the effects of fractal structure on competing first-order and second-order reactions ($A \rightarrow B$ and $A + A \rightarrow C$), involving the hypothetical chemical species A, B, and C, occurring at a catalyst surface. Due to the broad distribution in the accessibility of surface sites to substances diffusing from outside, it was demonstrated that fractal catalysts behave differently from smooth catalytic surfaces. In particular it was found that the dependence of the catalyst selectivity on the first-order rate constant exhibits a nonclassical power-law behaviour. This work was extended by Tambe *et al.* (6) to consider the effect of varying probability of reaction steps and rate constant on selectivity, and by Lee and Lee (7,8) who studied some of the effects of varying cluster size and fractal dimension. Elias-Kohav *et al.* (9) studied diffusion coupled with first-order reaction on two-dimensional random and fractal objects, noticing a distinct difference between the behaviour of the fractal and nonfractal objects. Coppens and Froment (10–14) have used a fractal model to study diffusion and reaction in amorphous catalyst particles and consider the consequences of fractal pore geometry on the performance of catalytic reactors. The model includes contributions from dead-end pores not usually included in network models. The Knudsen diffusivity derived for a fractal pore differs from that for a smooth, cylindrical pore and thus it was to be expected that the number of moles reacting per unit time in a fractal pore was not the same as the amount that would be calculated by applying the classical continuity and flux equations for components in a cylindrical pore. It is clear from this earlier work that if the catalyst pellets used in reactors possess fractal morphology and characteristics then this can mean that models based on more regular, Euclidean representations of the pore structure may give less accurate predictions of the catalyst and reactor behaviour.

METHODOLOGY

As mentioned above, Meakin (5), Tambe *et al.* (6), and Lee and Lee (7) have considered the dynamics of competing first- and second-order reactions at a surface modelled as a 2D DLA structure. Lee and Lee (7) studied the influence of varying the number of occupied lattice sites making up

[1] Present address: ICI Katalco, PO Box 1, Billingham, Cleveland, TS23 1LB, U.K. E-mail: sean_p_rigby@ici.com.

0021-9517/98 $25.00
Copyright © 1998 by Academic Press
All rights of reproduction in any form reserved.

the DLA cluster (here referred to as cluster mass) on the spatial distribution of a normalised selectivity within the cluster. The structures studied were of different size (i.e. spatial extent) and of the same fractal dimension. It was found that as the DLA size was decreased the selectivity probability was characterised by a wider distribution, showing a higher position sensitivity. This result was attributed to the fact that the outermost sites of the fractal object had a much higher selectivity for species C because the most exposed tips produce more bimolecular products, by the process $A + A \rightarrow C$, than the inner sites. It follows from this work that by tuning the controlling parameters in the growth of DLAs the resulting fractal objects may be made to have varying fractal dimensionality thereby offering the ability to control, or at least influence, selectivity. More recently, the same authors studied the effects on reaction selectivity of varying the fractal dimensionality in this way at fixed cluster mass. It was found that the selectivity towards the second-order process decreased with decreased fractal dimension. These observations were explained using the same reasoning as that applied to the influence of varying cluster mass at fixed fractal dimension; specifically the difference in the accessibility of the active sites to incoming random walkers. However, it is acknowledged by Lee and Lee (8) that the structures studied by them with the same cluster mass but differing fractal dimensions, also had different sizes (in the sense of linear spatial extent). This feature of these models means that the results cannot be interpreted to consider the influence of macroscopic heterogeneities in the spatial distribution of voidage and pore size in real three-dimensional pellets because the observed differences in the selectivity between reactions for these particular model structures might be attributed to solely an effect due to differences in overall average density. On probabilistic grounds alone a more dense cluster is bound to be less easily penetrated by a random walker; hence the influence of the difference in fractal dimension, and thus structural heterogeneity, has not strictly been deconvolved from the effect of average density variations. When considering the influence of comparitive density effects it is important, where fractal spatial scaling of mass is involved, to be specific about the length scales over which the density is measured. In this work we extend these studies to consider the same reaction scheme but occurring on three-dimensional (3D) cluster-cluster aggregate (CCA) mass fractal structures with a range of mass fractal dimensions and also a 3D Menger sponge. The topology of the structures (three-dimensional CCAs and Menger sponge) considered in this work is very different from that of the two-dimensional DLA structures considered in previous work (5–8) because the CCAs and Menger sponge possess an interconnected void space, as well as a fractal surface. This makes these structures more suitable than DLAs to study the influence of larger scale structural features of catalyst pellets on selectivity. Whereas the 2D DLAs with different numbers of occupied sites (known here as cluster mass) used in previous work (7) have differing spatial extents but the same fractal dimension and, thus, can be said to possess the same degree of heterogeneity, the 3D CCAs used in this work have the same spatial extent but different fractal dimensions, and hence, different degrees of heterogeneity. The aim of this work is to establish the relationship between selectivity and reaction probability, and the surface, pore, and catalyst pellet morphology and geometry.

The reaction mechanism described by the numerical algorithm used in this work is similar to that used by Tambe *et al.* (6) and is given by:

(i) $A + S \rightarrow A^*$
(ii) $A^* \rightarrow B$
(iii) $A + A^* \rightarrow C$.

Here, A represents the reacting particle, S is the fractal surface site, and B and C are the products. The selectivity is defined in this work as the ratio of the number of B molecules produced to that of C molecules produced. The case where steps (i) and (iii) occur with a probability of unity has been analysed by Meakin (5) on DLA and percolating clusters. In reality it is more likely that all the collisions may not be reactive. In the work of Tambe *et al.* (6) and the new work presented here certain probabilities for step (i) and (iii) were assumed and then the performance was simulated.

The simulations were carried out using a three-dimensional finite concentration CCA random fractal generated on a lattice of size $64 \times 64 \times 64$ sites following a method analogous to that described by Meakin (15) for creating 2D CCAs. Starting from a completely random cluster precursor, successively larger clusters are formed by the diffusion and aggregation of smaller units until only one unit remains. A typical 2D version of a CCA is shown in Fig. 1. The mass fractal dimensions for several 3D structures with different initial voidage fraction, ε ($=1 -$ fraction of lattice sites occupied by the cluster, ρ), determined using the "box-counting" method (16), is shown in Fig. 2. A value of the mass fractal dimension of 3 would imply that the structure of the cluster is homogeneous over the lengthscales from the size of the lattice unit to that of the whole lattice. A lower fractal dimension indicates an increasing degree of heterogeneity in the structure. The CCA itself was placed site for site at the centre of a lattice of size $74 \times 74 \times 74$ sites, which meant that a region of completely empty sites, of a depth of five lattice units, was left surrounding the CCA. In this context, cluster mass is defined as the number of occupied lattice sites. The cluster size is defined as its linear extent; in the case of all the CCAs used here the size was 64 lattice units. The bulk density of the structure is defined as the total number of occupied sites divided by the total number of sites in the minimum containing cubic lattice (identical to the creation lattice of $64 \times 64 \times 64$ sites for the CCAs in this

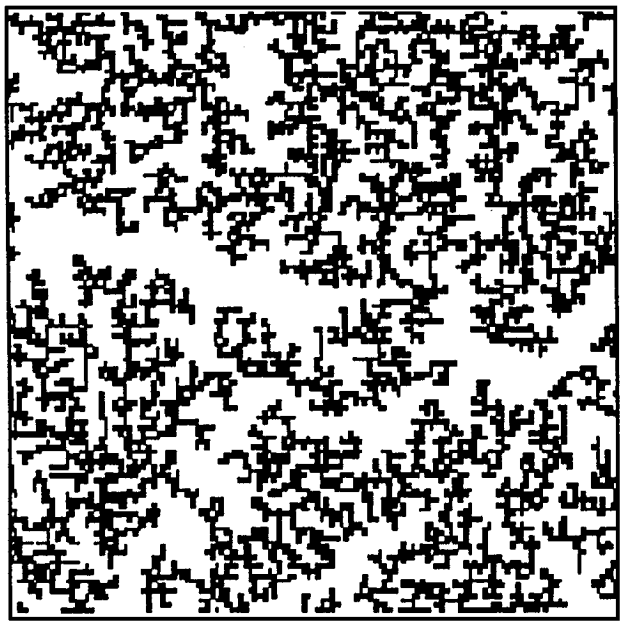

FIG. 1. Two-dimensional cluster-cluster aggregate (CCA) model structure. Lattice size 128 × 128 sites, voidage fraction = 0.65. Black indicates solid matrix; white indicates void space ((17); copyright Elsevier Science, 1996, reproduced with permission).

work). It then follows that the voidage fraction is defined as the ratio of the number of unoccupied sites to the total number of sites in the minimum containing lattice. This model structure was used to represent and study certain physical situations. First, the CCA structure could be used to model the large scale heterogeneity present in catalyst support pellets and thereby elucidate the effect that such heterogeneity has on selectivity. It has previously been suggested (17) that CCA fractals are a good model structure for the features of the macroscopic scale heterogeneities in the spatial distribution of voidage and pore size in real pellets that influence transport processes. Second, the CCA

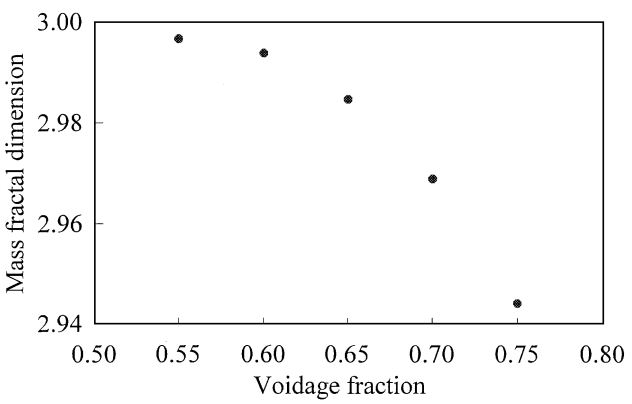

FIG. 2. Mass fractal dimensions (found by the "box-counting" method (16)) for three-dimensional CCA model structures.

structure could represent the microporous particle in a hierarchical structural model for bidisperse porous media of the type suggested by Ruckenstein *et al.* (18), Seaton (19), and Rolle-Kampczyk *et al.* (20). The outer void zone of the encompassing lattice would represent, in this case, the edge of the macropores, which are made up of the spacings between primary microporous particles. Third, the CCA could be envisaged, in a similar way to which a DLA was used by Meakin (5) and Tambe *et al.* (6), to represent the surface of a catalyst with a fractal shape because mass fractals are also surface fractals. The difference between these three situations is the length scale that the model represents. Fractal objects are characterised by self-similarity in geometry over all length scales.

In order to simulate the reaction, the following methodology was used: the probabilities of events (i) and (iii) were defined to be equal to P_1 and P_3, respectively. The molecule starts its random walk at a random site outside the area defined by the fractal boundaries. If this random-walking molecule comes onto a site occupied by the fractal cluster, it gets absorbed with probability P_1. Each molecule, prior to contact with a site on the CCA is assigned a random number (r) between 0 and 1. If $r < P_1$, then the molecule stays adsorbed, or continues its random walk (when $r > P_1$).

In the event when reaction (i) takes place, reaction (ii) follows and the number of B molecules produced (N_B) is increased by the product $k_2 N_{A^*}$. The term N_{A^*} refers to the total number of adsorbed A molecules on the fractal surface and k_2 denotes the rate constant for reaction step (ii). When N_B increases by the integer 1, a randomly chosen adsorbed A site is converted into a B molecule and the time also increments by 1. In this way, the rate constant for reaction (ii) is accounted for.

A randomly moving A molecule can also visit the fractal site on which an A molecule has already been adsorbed, in which case reaction (iii) takes place. A random number (r) is generated in the case of such an event and checked to see whether $r < P_3$, where P_3 is the probability of reaction (iii). If this check is positive, then the number of C molecules produced (N_C) and the time are incremented by 1, and the A molecule adsorbed at the site is said to have reacted with the moving A molecule. It is assumed for these simulations that the B and C molecules, once generated, desorb immediately.

All the sites occupied by the fractal cluster were considered reaction sites. When a moving A molecule travels sufficiently far away from the CCA cluster that it crosses the boundaries of the lattice, a periodic boundary condition, similar to that used for CCA generation is employed and the particle is returned at the equivalent site on the opposite face of the cubic lattice. In the simulations that have been carried out, a large number of A molecules were launched until the system attained a steady state. At this steady state the constant launching of A molecule random walkers is equivalent to a constant flux of A molecules hitting a site,

or sites, in the pore structure somewhere. The reactions producing *B* and *C* molecules proceed at a steady rate and the selectivity, as defined by the ratio N_B/N_C, may then be estimated. After the number of adsorbed *A* molecules reached a steady state the number of *B* and *C* molecules produced then grew linearly. It typically took 30,000–40,000 *A* molecule releases to reach a steady state. Approximately 400,000 trajectories of *A* molecules were considered. The selectivity presented, for a particular set of reaction parameters and a CCA of a particular mass (fundamentally related to a particular initial voidage fraction of the original lattice at cluster creation), represents the average result of simulations made on a number (typically 5) of CCAs of the same mass in order to give a reasonable degree of random error (typically 0.5%).

RESULTS

The value of k_2, the rate constant for reaction (ii), is taken to be equal to 0.0001 for all simulations. In addition to varying the values of P_1 and P_3, the number of occupied lattice sites making up the CCA clusters was also varied (equivalent to varying the voidage fraction in generating the CCA). The influence of the geometry of the cluster was studied by employing both CCA-type and Menger sponge fractal structures.

CCA Models

Figure 3 shows the variation in selectivity with the probability of second-order reaction, P_3, for CCAs of a particular cluster mass. The value of P_1 used in these simulations is 1.0. It can be seen that the selectivity for molecule *B* decreases as the probability of the second-order reaction increases as would be expected due to the enhanced production of *C* molecules. This is in general agreement with the findings of Tambe *et al.* (6) for similar processes on 2D DLAs.

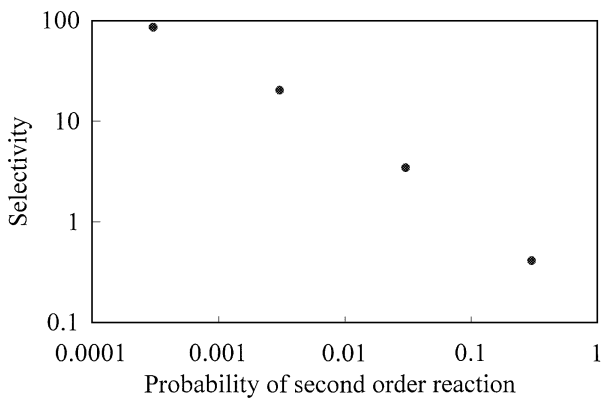

FIG. 3. Variation in selectivity (N_B/N_C) between competing first- and second-order reactions with the probability of second-order reaction (P_3) for 3D CCAs of initial voidage fraction in the original creation lattice equal to 0.75. Model parameter $P_1 = 1.0$.

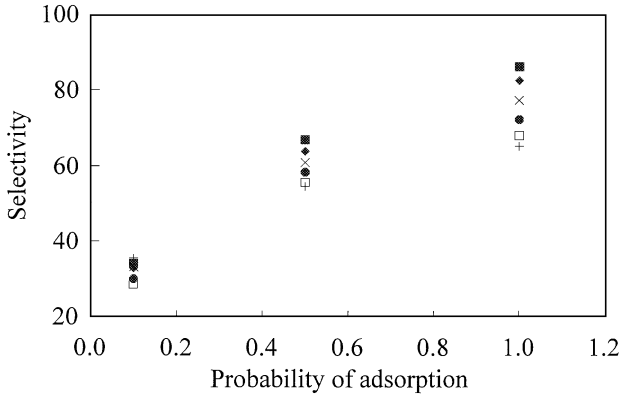

FIG. 4. Variation in selectivity (N_B/N_C) with varying probability of adsorption (P_1) for CCA model structures with six different voidage fractions (■, 0.75; ◆, 0.70; ×, 0.65; ●, 0.60; □, 0.55; +, 0.50) in the original creation lattice. Model parameters: P_1 = various, $k_2 = 0.0001$, $P_3 = 0.0003$.

Similar qualitative behaviour has also been observed for CCA models of different overall average voidage fraction; cluster voidage fractions in the range 0.5–0.75 have been investigated.

Figure 4 shows the variation in selectivity with the probability of adsorption, P_1, for CCA models with six different voidage fractions. P_3 was kept fixed at 0.0003. In general, selectivity for *B* increased with increased voidage fraction of the CCA and increased value of P_1. The relative difference in the selectivity for CCAs of different voidage fractions decreases at lower values of P_1. It has been suggested (7) that a lower P_1 value smooths out the screening effects due to model geometry because the active sites then come to possess nearly the same adhesive opportunity.

Comparison with the Menger Sponge Model

Figures 5, 6, and 7 show the variation in selectivity with varying cluster total mass, total surface area, and voidage

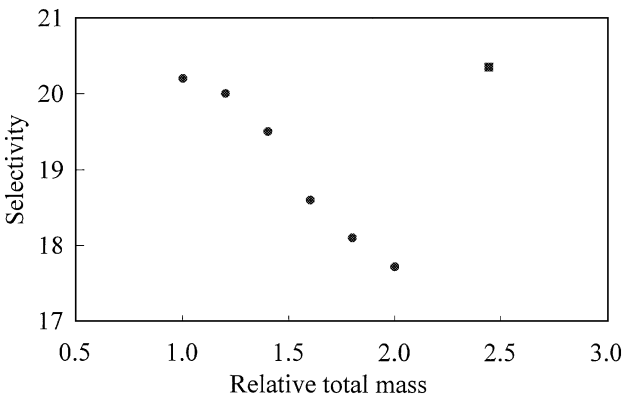

FIG. 5. A comparison of the variation in selectivity (N_B/N_C) with varying total cluster mass (relative to a CCA grown with an initial voidage fraction of 0.75 on the original creation lattice) for CCA (●) and Menger sponge (■) fractal model structures. Model parameters: $P_1 = 1.0$, $k_2 = 0.0001$, $P_3 = 0.003$.

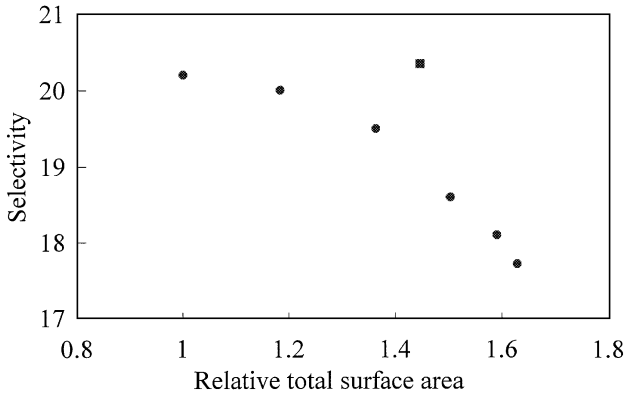

FIG. 6. A comparison of the variation in selectivity (N_B/N_C) with varying object total (internal and external) surface area (relative to a CCA grown with an initial voidage fraction of 0.75 on the original creation lattice) for CCA (●) and Menger sponge (■) fractal model structures. Model parameters: $P_1 = 1.0$, $k_2 = 0.0001$, $P_3 = 0.003$.

fraction, respectively, for CCA fractal model structures and a Menger sponge fractal. The parameters used in these simulations were $P_1 = 1.0$, $P_3 = 0.003$, and $k_2 = 0.0001$. The Menger sponge structure is created from an initial unit cube by taking out, or "coring," the middle thirds, where a "third" is a linear measure (1/3 of an edge length). This operation can be done readily over and over again, always scaling (linearly) by 1/3 of the previous construct and coring in the middle of the remainders. It is possible to evaluate the mass fractal dimension, d_m, of this object algebraically; hence,

$$d_m = \frac{\log 20}{\log 3} = 2.72. \qquad [1]$$

The fractal dimension of the Menger sponge structure is much lower than a CCA with an equivalent voidage fraction. The voidage fraction of the Menger sponge studied here was ~0.7. The original Menger sponge used in these simulations had an overall sidelength for the minimum containing cubic lattice of 81 lattice units. The lowest allowable "pore size" was one lattice unit. This lattice size was chosen such that it allowed, by a consideration of the combined results for CCAs and the Menger sponge in Figs. 5, 6, and 7, a study of the influence on reaction selectivity of all of the parameters: model total mass, total surface area, and voidage fraction. For the purposes of the selectivity Monte-Carlo simulations a void zone five lattice units deep was added on all sides of the Menger sponge itself, similar to the simulation lattice construction used for the 3D CCA.

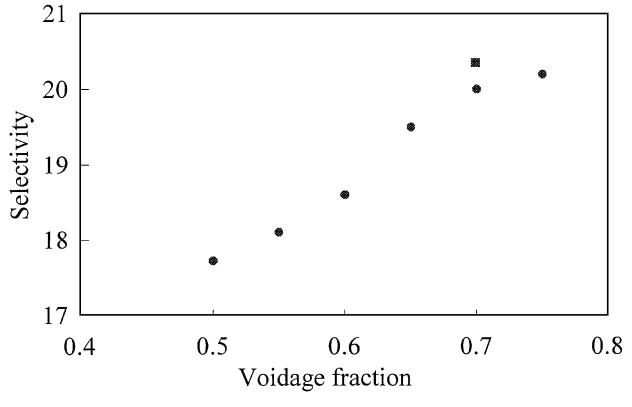

FIG. 7. A comparison of the variation in selectivity (N_B/N_C) with varying voidage fraction for CCA (●) and Menger sponge (■) fractal model structures. Model parameters: $P_1 = 1.0$, $k_2 = 0.0001$, $P_3 = 0.003$.

It can be seen from Figs. 5 and 6 that there is a general trend of decreasing selectivity towards species *B* with increased CCA cluster total mass and total surface area. From Fig. 7 it can be seen that for CCA clusters selectivity increases with increased voidage fraction. A comparison of these results for CCA clusters, in general, with the respective results for the Menger sponge shows that the Menger sponge does not fit in with these observed general trends, irrespective of whether selectivity is correlated with cluster total mass, total surface area, or voidage fraction. However, it is clear from Fig. 7 that the selectivity for the Menger sponge structure is relatively closer to the general trend for CCA structures when correlated with voidage fraction. This observation would suggest that the overall average voidage fraction of the structure is likely to be a major contributory factor to the selectivity but the existence of the relatively small, but significant, discrepancy in Fig. 7 between the selectivity for the Menger sponge and the trend in the CCA data suggests that a further feature of the cluster structure is also important in determining selectivity.

A consideration of the CCA results in Figs. 5, 6, and 7, in combination with those in Fig. 2, suggests that the selectivity for *B* is favoured by structures with lower mass fractal dimension. Figures 5, 6, and 7 suggest greater selectivity for *B* from lower total mass CCA structures which also have lower surface area and higher voidage fraction. However, this result might be attributed purely to the overall mass, surface area, or voidage fraction of the structure. The results for the Menger sponge show that it has a much higher selectivity for *B* than might be anticipated merely from extrapolation of the results for the CCA structures on the grounds of cluster mass, or total surface area, or even voidage fraction. This would seem to suggest that in this case higher selectivity for *B* is, indeed, associated with lower fractal-dimensional structures and not just solid particle (cluster) mass or surface area, or the voidage fraction. This supposition is confirmed by Fig. 8, which shows reaction selectivity against mass fractal dimension of the structure. In Fig. 8 the result for the Menger sponge fits in well with a general trend of increasing selectivity with decreasing mass fractal dimension. However, the rate of change of selectivity with mass fractal dimension decreases with decreasing fractal dimension, particularly for mass fractal dimensions less than ~2.95. This result would suggest that the further feature

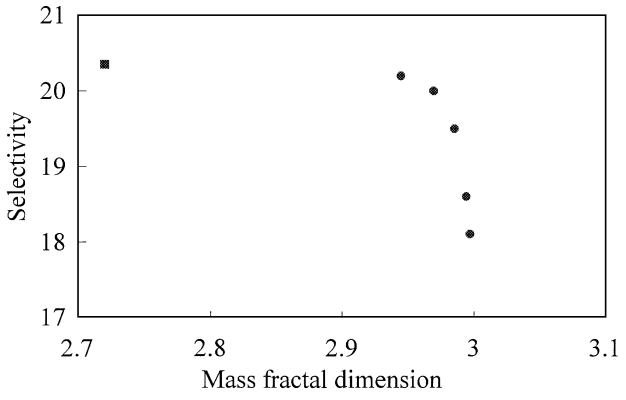

FIG. 8. Variation of reaction selectivity with the mass fractal dimension of the model structure for CCA (●) and Menger sponge (■) fractals. Model parameters: $P_1 = 1.0$, $k_2 = 0.0001$, $P_3 = 0.003$.

of the model structure determining selectivity, in addition to overall average voidage fraction, is characterised by the mass fractal dimension.

DISCUSSION

If the combined results for CCA-type structures and the Menger sponge shown in Figs. 5–8 are considered it is clear that an explanation for the observed trends for the CCA clusters, based purely on the effect of changes in the overall bulk density, is inadequate. The Menger sponge result in Fig. 7 clearly conflicts with this simple rationalisation because it does not fit in with the trend in the CCA data. However, a more universal relationship between reaction selectivity and cluster structure characteristics may be established by considering the correlation of selectivity with mass fractal dimension and the particular features of a model structure characterised by a mass fractal dimension. The mass fractal dimension characterises how the solid is distributed in space and how rapidly convolutions in the structure repeat themselves at ever changing lengthscales. In contrast to the result for the Menger sponge, the trends in the selectivity results for CCAs are similar to what might be expected for more uniform clusters, consistent with the mass fractal dimensions of the CCAs studied in this work being relatively close to a value of 3. A mass fractal dimension of 3 is the expected value for a uniform structure. For a fixed lattice size, less significant rearrangement from a random cluster precursor is required to produce a CCA from a higher mass density random cluster than for a lower mass density random cluster. Therefore, the lower total mass CCA fractals studied here, first, tend to be more heterogeneous than their random cluster precursors of equivalent total mass and, second, tend to be more heterogeneous than CCA structures of higher total mass. This second point is clear from Fig. 2, where CCAs of low voidage fraction have higher mass fractal dimensions than CCAs of a higher voidage fraction, because a lower fractal dimension is associated with a more heterogeneous structure. The Menger sponge may be considered to be a more heterogeneous structure still, as it has a lower mass fractal dimension than any of the CCA models considered.

For lattice-based models, such as the Menger sponge, the voidage fraction, ε, of the lattice is related to the mass fractal dimension, d_m, of the cluster occupying that lattice via the relation

$$\varepsilon = 1 - \left(\frac{E_1}{E_2}\right)^{3-d_m}, \qquad [2]$$

where E_1 and E_2 are the lower (equal to one lattice unit) and upper (equal to the lattice size) lengthscale cutoffs. For the structures studied here E_1/E_2 equals 1/81 for the Menger sponge and 1/64 for the CCAs. It should be noted that if a ramification, by a further level, of the Menger sponge structure studied above had been used, while the value of d_m would have remained constant, the values of voidage fraction and E_1/E_2 would have varied. The results of the Monte-Carlo simulations presented here show that both voidage fraction and mass fractal dimension influence selectivity. This would suggest that the lengthscale, i.e. linear extent (explicitly related to the voidage fraction via Eq. [2]) for the model is also important. These results have shown that the characteristics of the (fractal) model that need to be related to those obtained from the characterisation data, such as MRI, for a real material are two of mass fractal dimension, voidage fraction, or linear extent, together. In the two-dimensional studies reported previously (8) the linear extent of the model varied at the same time as the fractal dimension was also varied, and thus the results obtained here would suggest that that study did not deconvolve the effects due to different linear extent from those due to varying fractal dimension. As mentioned above, it is the purpose of the new work reported here to identify the characteristics of a model of a real porous material that are necessarily required for that model to *adequately* represent that real material.

CONCLUSIONS

The work described here highlights the essential requirement to identify the characteristics of a model that need to be related to the properties of real materials, if a model is to correctly represent a given real material. In the past other workers have simply reported results for abstract numerical models, while the new work presented here is a first step in trying to develop and select modelling strategies that are constrained by input from experimental characterisation data. Three-dimensional models are obviously a much better representation of real materials than two-dimensional models. The simulations described here suggest that voidage fraction (which for the three-dimensional models

considered here is inherently related to linear extent) and mass fractal dimension are both important parameters that influence selectivity. These new results suggest that the particular influence of both these effects was not explicitly clear in the previous results for two-dimensional models.

ACKNOWLEDGMENTS

SPR thanks EPSRC for financial support and ICI and The Royal Academy of Engineering for the award of an ICI scholarship.

REFERENCES

1. Hollewand, M. P., and Gladden, L. F., *J. Catal.* **144**, 254 (1993).
2. Hollewand, M. P., and Gladden, L. F., *Chem. Engng Sci.* **50**, 327 (1995).
3. Rigby, S. P., Cheah, K.-Y., and Gladden, L. F., *Appl. Catal. A* **144**, 377 (1996).
4. Pfeifer, P., and Avnir, D., *J. Chem. Phys.* **79**, 3558 (1983).
5. Meakin, P., *Chem. Phys. Lett.* **123**, 428 (1986).
6. Tambe, S. S., Badola, P., and Kulkarni, B. D., *Chem. Phys. Lett.* **173**, 67 (1990).
7. Lee, C.-K., and Lee, S.-L., *Chem. Phys. Lett.* **226**, 88 (1994).
8. Lee, C.-K., and Lee, S.-L., *Surf. Sci.* **339**, 171 (1995).
9. Elias-Kohav, T., Sheintuch, M., and Avnir, D., *Chem. Engng Sci.* **46**, 2787 (1991).
10. Coppens, M.-O., and Froment, G. F., *Chem. Engng Sci.* **49**, 4897 (1994).
11. Coppens, M.-O., and Froment, G. F., *Chem. Engng Sci.* **50**, 1013 (1995).
12. Coppens, M.-O., and Froment, G. F., *Chem. Engng Sci.* **50**, 1027 (1995).
13. Coppens, M.-O., and Froment, G. F., *Chem. Engng Sci.* **51**, 2283 (1996).
14. Coppens, M.-O., and Froment, G. F., *Chem. Engng J.* **64**, 69 (1996).
15. Meakin, P., *Phys. Rev. Lett.* **51**, 1119 (1983).
16. Mandelbrot, B. B., "The Fractal Geometry of Nature." Freeman, New York, 1982.
17. Rigby, S. P., and Gladden, L. F., *Chem. Engng Sci.* **51**, 2263 (1996).
18. Ruckenstein, E., Vaidyanathan, A. S., and Youngquist, G. R., *Chem. Engng Sci.* **26**, 1305 (1971).
19. Seaton, N. A., *Chem. Engng Sci.* **46**, 1895 (1991).
20. Rolle-Kampczyk, U., Karger, J., Caro, J., Noack, M., Klobes, P., and Rohl-Kuhn, B., *J. Colloid Interface Sci.* **159**, 366 (1993).